Measurement of backward sputtering yields induced by fast neutrons

Bangjiao Ye [a,*], Yoshimi Kasugai [b], Yujiro Ikeda [b], Yangmei Fan [a], Jiangfeng Du [a], Xianyi Zhou [a], Rongdian Han [a]

[a] *Department of Modern Physics, University of Science and Technology of China, Hefei, Anhui 230026, People's Republic of China*
[b] *Japan Atomic Energy Research Institute, Tokai, Naka, Ibaraki, Japan*

Abstract

This paper presents experimental methods and results of measuring backward sputtering induced by fast neutrons. Backward sputtering yields of 10 materials Mg, Al, Sc, V, Fe, Co, Cu, Zr, Au and type 316 stainless steel have been measured and compared with forward sputtering yields. The typical value of backward sputtering yield is about 10^{-8}–10^{-10} atoms per neutron, which is approximately 1–2 orders smaller than that of forward sputtering. The present results have been compared with other experimental results and have been explained using sputtering theories. © 2000 Elsevier Science B.V. All rights reserved.

1. Introduction

When energetic neutrons bombard a solid and their energy is transferred to surface or near-surface atoms, sputtering can occur. D + T neutrons have a sufficient energy to induce nuclear reactions such as (n, 2n), (n, p), (n, α) and (n, np). Some of the recoil nuclei have enough amount of energy to be emitted from the surface. Neutron sputtering will introduce atoms from the solid wall of the plasma chamber into the hot deuterium–tritium plasma [1,2] and lead to the emission of radioactive wall atoms into the coolants of the cooling system [3]. Neutron sputtering will also contribute to erosion of the vessel walls [4]. Most of the experimental measurements and theoretical treatments for neutron sputtering yields were carried out in the 1970s. The most extensive sputtering yield measurements have been performed for Nb [5,6] and Au [7,8] materials. Sputtering yield results for Au and Nb vary from the order of 10^{-5} to 0.25 atoms per neutron. Most of the measurements supplied only the forward sputtering yields and very few groups obtained the backward sputtering yield. During 1996 and 1997, we made a systematic study of sputtering yields for 24 materials [9]. The systematics for reduced sputtering yields (RS_n), that is, sputtering yields divided by the cross-section of reaction, have been found [10]. All experimental data of RS_n for forward sputtering can be predicted by a simple power function $RS_n = aZ^b$, where a and b were the fitting parameters and Z was the atomic number of the recoil nucleus.

As neutrons can penetrate though a solid with a large thickness, sputtering can occur on both sides of the target. Backward sputtering occurs when the recoil nuclei are emitted in the backward direction relative to the direction of neutron incidence. The large forward sputtering yield relative to the backward sputtering yield for energetic neutrons is caused by isotropic scattering, which strongly favors energy transfer in the forward direction. During the experimental measurement of the systematics of sputtering yields, we have also obtained the backward sputtering of 10 materials with 11

---

[*] Corresponding author. Tel.: +86-551 360 1164; fax: +86-551 360 2985.
E-mail address: bjye@ustc.edu.cn (B. Ye).

reactions such as (n, 2n), (n, α) and (n, p). This paper presents the experimental results of backward sputtering yields and compared with forward sputtering yields.

2. Experimental procedures

Because sputtering yields by neutrons are generally very low, it is very important to select suitable materials and reactions. The cross-sections of the reaction and the half-life of the recoiled particles should be considered synthetically. We chose 24 kinds of materials to study the systematics, but backward sputtering yield was only measured in 10 kinds of materials, such as magnesium, aluminum, scandium, vanadium, iron, cobalt, copper, zirconium, gold and SS316. All samples were bought from the Goodfellow Company. The thickness of the target foil was from 0.005 to 0.25 mm and the size of the target was 25×25 mm^2. In order to perform well-defined sputtering measurements, the surfaces of the target to be investigated should be extremely carefully cleaned to avoid any surface debris or loosely bound microparticles being knocked off the target and reaching the collectors.

The present measurement was performed in air. For this method, we need to measure the change of activity at the collector with distance between the target and the collector. The collectors for collecting the sputtering materials were made from plastic film. Most of the collectors were first cut to 2.5×2.5 cm^2 size. The thickness of each collector was 0.013 mm. A plastic ring was made specially as the holder to fix the collector and

the target. Each target–collector assembly consisted of one target, two collectors and two plastic holders as shown in Fig. 1. The thickness of the holder was 0.2, 0.5, 1.0, 2.0, 3.0 and 5.0 mm, which separated the target from the collectors. For each material studied, 4–6 target–collector assemblies were prepared and loaded in a cylindrical plastic tube as a target–collector stack.

14.9 MeV neutrons were produced by T(d, n) reaction at the neutron generator of the Fusion Neutronics Source (FNS), Japan Atomic Energy Research Institute (JAERI). Two round experiments were conducted in a rotational target room, utilizing the FNS heavy irradiation machine time at an average neutron flux of 2.2×10^{12} n/s. The other two round experiments were carried out in an 80° target room at the average neutron flux of 1.5×10^{11} n/s. The target–collector stack was placed at a distance of 10–50 mm from the neutron source in a direction of 0° with respect to the d$^+$ beam. The irradiation time was chosen according to the half-lives of the reactions. Excepting the ^{27}Al(n, p)^{27}Mg reaction, for which the sample was only irradiated for 10 min, some samples were irradiated for 7–30 h. A schematic of the irradiation configuration is given in Fig. 1.

After irradiation, the experimental target–collector stack was disassembled. The collector was cut carefully from the holder to avoid possible loss of sputtered material. γ-rays from the irradiated samples and the sputtered materials deposited in the collectors were measured using four germanium detectors. A type γ-ray spectrum of radioactivity in the collector sputtered from the niobium target is shown in Fig. 2. One germanium detector was used as the standard detector for which the
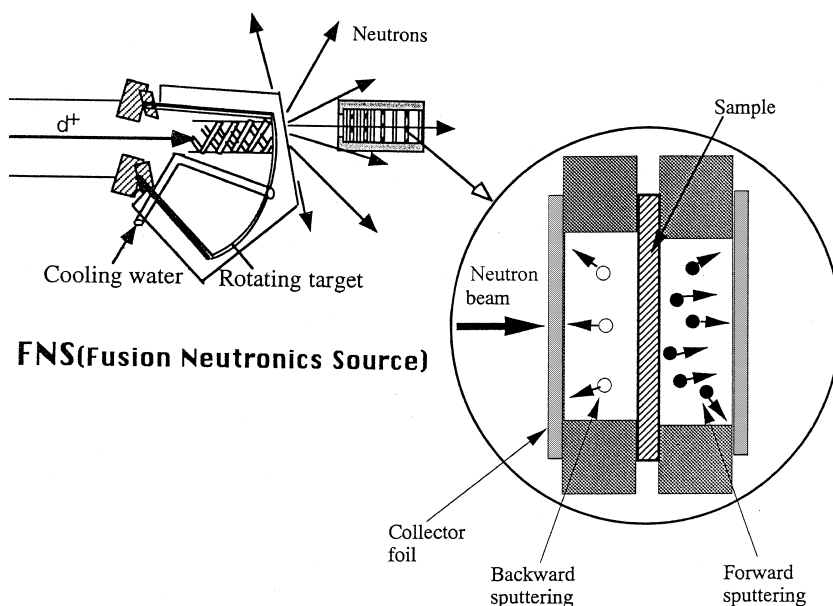

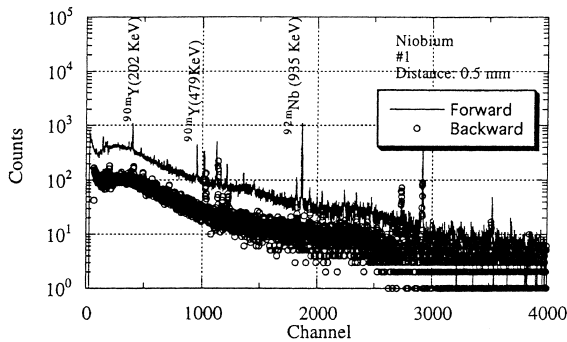Fig. 1. Experimental configuration for measuring fast neutron sputtering yields.

Fig. 2. Gamma-ray spectra of radioactivity in the collector in the case of sputtering from the niobium target irradiated with 14.9 MeV neutrons.

detection efficiency has been calibrated carefully. The other detectors were used to measure relative γ-ray yields. The efficiencies of the relative detectors were calibrated for each γ-ray peak by measuring the same sample with both relative and standard detectors.

3. Result and discussion

The neutron sputtering yields were estimated by extrapolating the data at different distances to 0 mm distance. Figs. 3–5 show backward sputtering yields in different distances and the fitting curves for (n, α), (n, p) and (n, 2n) reactions, respectively. In the present measurement, the activities of eleven reactions at the collectors were measured. Some of the backward sputtering yields were measured using two or three collectors because of very weak activities. The fitting results for backward sputtering yields at the target surface are shown in Table 1. The error is composed of two parts:
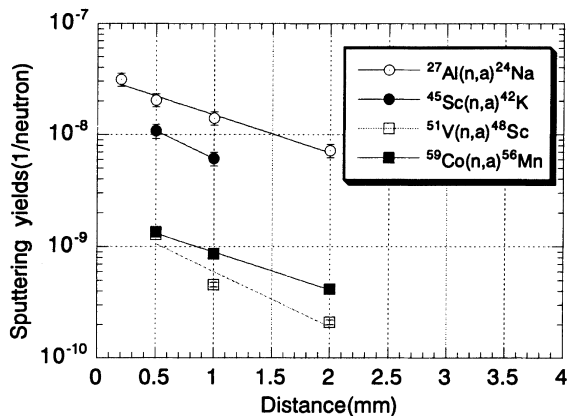

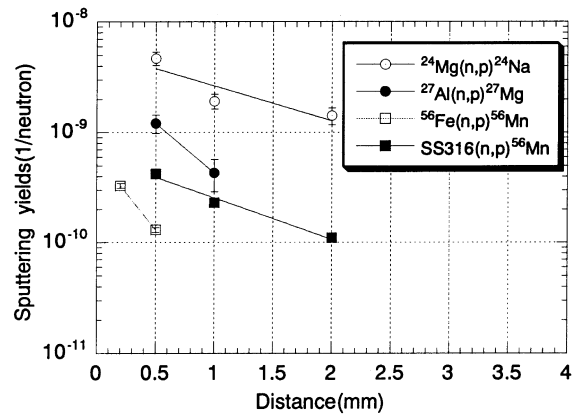Fig. 3. Backward sputtering yields at different distances for (n, α) reactions.

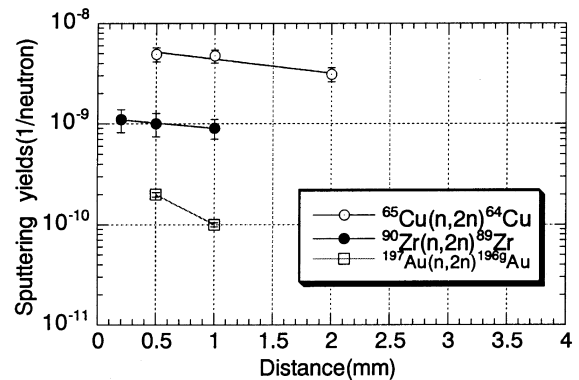Fig. 4. Backward sputtering yields at different distances for (n, p) reactions.

Fig. 5. Backward sputtering yields at different distances for (n, 2n) reactions.

one is the statistical error for the peak count and the other is identified to be systematic error.

For comparison, the forward sputtering yields for the same reaction are also listed in Table 1. In the present work, the backward sputtering yields are a factor of 5–200 lower than that of the forward ones depending on the target materials. We can postulate that the ratios S_f/S_b, that is, the ratios between the forward sputtering yield (S_f) and the backward sputtering yield (S_b), depend on reaction types, for example, 24–180 for (n, p) and (n, 2n) reactions and 5–20 for the (n, α) reaction as shown in Table 2. The experimental results of Harling [11] have also been listed in Table 2.

Most of the theories for fast neutrons are transplanted and developed from the ion sputtering theory of Sigmund [12]. According to the theory of sputtering by fast neutrons [13], S_f/S_b is given by

$$\frac{S_f}{S_b} = \frac{\langle R_f \rangle}{\langle R_b \rangle R_N}, \tag{1}$$

Table 1
Backward sputtering yields induced by fast neutrons

Reactions	σ (mb)	S_b (1/neutron)	S_f (1/neutron)
^{24}Mg(n, p)^{24}Na	168	$5.47 \times 10^{-9} \pm 7.01 \times 10^{-10}$	$9.46 \times 10^{-7} \pm 1.11 \times 10^{-7}$
^{27}Al(n, p)^{27}Mg	62.3	$3.42 \times 10^{-9} \pm 6.80 \times 10^{-10}$	$2.82 \times 10^{-7} \pm 3.67 \times 10^{-8}$
^{56}Fe(n, p)^{27} ^{56}Mn	111	$6.11 \times 10^{-10} \pm 1.90 \times 10^{-10}$	$5.84 \times 10^{-8} \pm 7.60 \times 10^{-9}$
SS316(n, p)^{56}Mn	111	$3.64 \times 10^{-10} \pm 7.27 \times 10^{-11}$	$3.79 \times 10^{-8} \pm 5.69 \times 10^{-9}$
^{27}Al(n, α)^{24}Na	114	$3.27 \times 10^{-8} \pm 4.80 \times 10^{-9}$	$6.62 \times 10^{-7} \pm 8.59 \times 10^{-8}$
^{45}Sc(n, α)^{42}K	53.3	$1.92 \times 10^{-8} \pm 3.00 \times 10^{-9}$	$9.52 \times 10^{-8} \pm 1.24 \times 10^{-8}$
^{51}V(n, α)^{48}Sc	16.9	$1.89 \times 10^{-9} \pm 3.00 \times 10^{-10}$	$2.11 \times 10^{-8} \pm 2.79 \times 10^{-9}$
^{59}Co(n, α)^{56}Mn	32.3	$1.92 \times 10^{-9} \pm 2.50 \times 10^{-10}$	$3.57 \times 10^{-8} \pm 4.65 \times 10^{-9}$
^{65}Cu(n, 2n)^{64}Cu	961	$6.10 \times 10^{-9} \pm 1.10 \times 10^{-9}$	$1.77 \times 10^{-7} \pm 2.50 \times 10^{-8}$
^{90}Zr(n, 2n)^{89}Zr	832	$1.02 \times 10^{-9} \pm 2.80 \times 10^{-10}$	$5.78 \times 10^{-8} \pm 7.54 \times 10^{-9}$
^{197}Au(n, 2n)^{196g}Au	1894	$2.42 \times 10^{-10} \pm 4.50 \times 10^{-11}$	$1.16 \times 10^{-8} \pm 1.62 \times 10^{-9}$

Table 2
The ratios between forward sputtering yields and backward sputtering yields

Reactions	Q-values (MeV)	T-forward (keV)	T-backward (keV)	S_f/S_b present work	S_f/S_b Harling	S_f/S_b calculation
^{27}Al(n, α)^{24}Na	−3.13	1390	770	20	–	24
^{45}Sc(n, α)^{42}K	−0.4	1290	750	5	–	23
^{51}V(n, α)^{48}Sc	−2.06	1220	680	11	17	24
^{54}Fe(n, α)^{51}Cr	0.848	1240	740	–	15	22
^{62}Ni(n, α)^{59}Fe	−0.441	1190	690	–	6	23
^{50}Ti(n, α)^{47}Ca	−3.437	1210	650	–	10	24
^{63}Cu(n, α)^{60}Co	1.715	1220	740	–	11	22
^{59}Co(n, α)^{56}Mn	0.33	1220	720	19	–	23
^{24}Mg(n, p)^{24}Na	−4.73	1170	–	173	–	–
^{27}Al(n, p)^{27}Mg	−1.83	1180	–	83	–	–
^{56}Fe(n, p)^{56}Mn	−2.91	980	–	96	–	–
^{54}Fe(n, p)^{54}Mn	0.089	1020	40	–	24	140
SS316(n, p)^{54}Mn	−2.91	980	–	104	–	–
^{58}Ni(n, p)^{58}Co	0.392	1000	82	–	88	85
^{92}Mo(n, p)^{92m}Nb	0.274	900	75	–	49	83
^{52}Cr (n, 2n)^{51}Cr	−12.04	910	–	–	134	–
^{55}Mn(n, 2n)^{54}Mn	−10.22	950	–	–	139	–
SS316(n, 2n)^{51}Cr	−12.04	910	–	–	96	–
^{65}Cu(n, 2n)^{64}Cu	−9.91	920	–	29	–	–
^{90}Zr(n, 2n)^{89}Zr	−11.98	800	–	57	–	–
^{93}Nb(n, 2n)^{92m}Nb	−8.82	870	–	–	140	–
^{100}Mo(n, 2n)^{99}Mo	−8.30	860	–	–	179	–
^{197}Au(n, 2n)^{196g}Au	−8.07	730	–	48	37	–

where R_N is the coefficient of energy reflection, which is known to be about 1/20 for fast neutrons [13], $\langle R_f \rangle$ and $\langle R_b \rangle$ are the mean projected ranges of the recoil nucleus for forward and backward directions, respectively. According to Schiott [14], the mean projected range of a primary knock-on atom starting with T in a solid in a direction θ relative to the surface normal is given by

$$\langle R(T) \rangle \; (\mu g/cm^2)$$
$$= \begin{cases} C_l A_2 \left(\dfrac{Z_1^{2/3} + Z_2^{2/3}}{Z_1 Z_2} T \; (keV) \right)^{2/3}, & \varepsilon < 0.1, \\ C_i A_2 \dfrac{(Z_1^{2/3} + Z_2^{2/3})^{1/2}}{Z_1 Z_2} T \; (keV), & 0.5 < \varepsilon < 10, \end{cases} \quad (2)$$

where ε is defined as a reduced energy [14] and A_1, A_2, Z_1 and Z_2 are the mass number and atomic number of target and recoil nuclei, respectively. C_l and C_i are the coefficients as shown in Figs. 4 and 7 of [14].

For the reaction induced by fast neutrons, according to nuclear reaction kinetics, the kinetic energy of the recoil nucleus is

$$T = \left\{ \frac{(A_2 E_n)^{1/2}}{A_{CN}} \cos\theta \pm \left(\frac{A_2 E_n}{A_{CN}^2} \cos^2\theta + \frac{A_{LP} Q + E_n(A_{LP} - 1)}{A_{CN}} \right)^{1/2} \right\}^2, \quad (3)$$

where A_{CN}, A_2 and A_{LP} are the mass numbers of compound nuclei, recoil nuclei and light nuclei which are emitted from compound nuclei, respectively. Q is the reaction Q-value. In order to give a basic conclusion, we let θ be equal to 0° for forward sputtering and to 180° for backward sputtering. For (n, α) reaction, the kinetic energy predicted theoretically for backward recoil nuclei is about 3/5 of that of forward recoil nuclei. For (n, p) reactions with negative Q values the recoil nuclei can never be projected in the backward direction. For a few (n, p) reactions with positive reaction values, the recoil kinetic energy are very small. For all (n, 2n) reactions studied here with the negative Q values, the recoil nuclei cannot be projected in the backward direction. The calculated results are also listed in Table 1. For (n, α) reactions, the S_f/S_b are calculated to be about 23, which is a little larger than that of experimental results of 5–20. This is due to the cascading processes of fast neutrons which also cause the additional backward sputtering. The same situation occurs for (n, p) and (n, 2n) reactions. We can still measure the backward yields, although very few or no nuclei were sputtering in backward direction according to the theoretical prediction. The experiment shows the values of S_f/S_b for (n, p) and (n, 2n) reactions were much smaller than those of (n, α) reactions.

4. Summary

The backward sputtering yields induced by fast neutrons have been measured for 10 materials. The experimental results show that the backward sputtering yields are about 1–2 orders smaller than those of forward sputtering, which have also been explained by the sputtering theories of fast neutrons. The backward sputtering yields depend on the kinetic energy of the recoil nuclei. Non-zero backward sputtering yields for (n, 2n) and (n, p) reactions are found in the present experiment. This is induced by multiple collisions. For the same atomic number, the backward sputtering yields for (n, α) reactions are generally larger than those for (n, p) and (n, 2n) reactions.

References

[1] R. Behrisch (ed.), Sputtering by Particle Bombardment II, Topics in Applied Physics, vol. 52, Springer, Berlin, Heidelberg, New York, 1983.

[2] W. Eckstein, J. Nucl. Mater. 248 (1997) 1.

[3] G. Cambi, D.G. Cepraga, S. Ciattaglia, L.D. Pace, G. Cavallone, Fus. Eng. Des. 29 (1995) 207.

[4] C. Garcia-Rosales, J. Nucl. Mater. 211 (1994) 202.

[5] R. Behrisch, O.K. Harling, M.T. Thomas, R.L. Brodziniski, L.H. Jenkins, G.J. Smith, J.F. Wendelken, M.J. Saltmarch, M. Kaminsky, S.K. Das, C.M. Logan, R. Meisenheimer, J.E. Robinson, M. Shimotomai, D.A. Thompson, J. Appl. Phys. 48 (1977) 3914.

[6] R.G. Meisenheimer, J. Vac. Sci. Technol. 14 (1977) 560.

[7] O.K. Harling, M.T. Thomas, R.L. Brodzinski, L.A. Rancitelli, Phys. Rev. Lett. 34 (1977) 1340.

[8] M.A. Kirk, R.A. Conner, D.G. Wozniak et al., Phys. Rev. B 19 (1979) 87.

[9] B.J. Ye, Y. Kasugai, Y. Ikeda, JAERI-Research, 1997, 97-082.

[10] B.J. Ye, Y. Kasugai, Y. Ikeda, Y.M. Fan, X.Y. Zhou, J.F. Du, R.D. Han, J. Appl. Phys. 87 (2000) 2581.

[11] O.K. Harling, M.T. Thomas, R.L. Brodziniski, L.A. Rancitelli, J. Appl. Phys. 48 (1977) 4328.

[12] P. Sigmund, Phys. Rev. 184 (1969) 383.

[13] R. Behrisch (ed.), Sputtering by Particle Bombardment I, Topics in Applied Physics, vol. 47, Springer, Berlin, Heidelberg, New York, 1981 (Chaps. 2–3).

[14] H.E. Schiott, Radiat. Eff. 6 (1970) 107.